FEBRUARY 1980 PPPL-1627
UC-20g

INTEGRAL EQUATION ANALYSIS OF DRIFT WAVE EIGENMODES IN A SHEARED SLAB GEOMETRY

BY

W. M. TANG, G. REWOLDT,
AND E. A. FRIEMAN

PLASMA PHYSICS LABORATORY

PRINCETON UNIVERSITY
PRINCETON, NEW JERSEY

This work was supported by the U. S. Department of Energy Contract No. EY-76-C-02-3073. Reproduction, translation, publication, use and disposal, in whole or in part, by or for the United States Government is permitted.

Integral Equation Analysis of Drift Wave Eigenmodes in a Sheared Slab Geometry

W. M. Tang, G. Rewoldt, and E. A. Frieman

Plasma Physics Laboratory, Princeton University,

Princeton, New Jersey 08544

The derivation of the appropriate form for the integral eigenmode equation governing both electron and ion drift waves of arbitrary radial wavelengths in a sheared slab is presented. The solutions to this equation provide useful information regarding the absolute stability of universal modes and ion-temperature-gradient driven modes for arbitrary wavelengths, and particularly for short wavelengths.

I. INTRODUCTION

The investigation of the stability of drift waves in a sheared slab geometry has been actively pursued in numerous recent publications.[1-3] These calculations have dealt with long radial wavelength eigenmodes governed by a differential equation of the form

$$[\rho_i^2 \partial^2/\partial x^2 + Q(x,\omega)]\tilde{\phi}(x) = 0 \quad , \tag{1}$$

with ρ_i being the ion gyroradius and $Q(x,\omega)$ being the radial potential whose specific form is determined by the particular instability considered. However, at shorter radial wavelengths, where the assumption $|\rho_i^2 \partial^2/\partial x^2| << 1$ breaks down, it becomes necessary to deal with the integral equation generalization of Eq. (1). The present paper is concerned with the derivation of the appropriate form of this integral eigenmode equation and with obtaining solutions for both electron and ion drift waves.

Results from the differential eigenmode equation studies have indicated that as the azimuthal wave number (k_y) is increased to $k_y\rho_i \sim 1$, the radial localization of the mode becomes of the order of the ion gyroradius. For electron drift waves,[1] this is a consequence of the fact that as $k_y\rho_i$ is increased, there is a downward shift of the eigenfrequency caused by finite gyroradius effects; i.e., $\omega = \omega_{*e} I_o(b_y)\exp(-b_y)$ with $b_y = k_y^2\rho_i^2/2$ and I_o being the familiar Bessel function. Since the radial position, where ion-Landau damping becomes dominant, is proportional to ω (i.e., $\omega \approx k_\parallel v_i$ with v_i being the ion thermal

velocity and $k_{\parallel} \propto x$ for a sheared slab), the corresponding radial localization of the eigenmode is also shifted to smaller values. Hence, it is of interest to apply the proper integral equation analysis to examine the stability properties of these waves at shorter wavelengths.

In the case of ion drift waves,[2,3] the radial localization of the eigenmodes is again determined by the ion-Landau resonance region. Differential equation eigenmode studies of ion-temperature-gradient-driven instabilities of this branch indicate that the largest growth rates are found for waves with $k_y \rho_i$ approaching one with corresponding eigenmodes localized to a radial extent of a few ion gyroradii.[2,3] Since the dominant part of the unstable spectrum here falls in the regime of wavelengths where the differential eigenmode equation is breaking down, it becomes important to generalize the calculation to an integral equation analysis appropriate at arbitrary wavelengths.

Motivated by the preceding considerations, we present a systematic derivation of the integral eigenmode equation of interest in Sec. II. In this section the procedures employed to solve the resultant equation are also described. Results from the computer code implementing the integral equation formalism ("integral formulation code") are presented in Sec. III for collisionless electron drift waves ("universal" modes), and in Sec. IV for the ion-temperature-gradient-driven ion drift instabilities. Finally, we conclude with a brief summary and general comments in Sec. V.

II. Derivation of Integral Eigenmode Equation

The form of the integral equation governing collisionless electrostatic drift waves for arbitrary $k_x \rho_i$ in a sheared slab geometry is derived in this section. Assuming that there is no equilibrium electric field, the governing equation for the perturbed distribution function f (given, for example, in Ref. 4) reduces to:

$$\frac{\partial f}{\partial t} + \underset{\sim}{v}\cdot\nabla f - \frac{e}{m}\nabla\Phi\cdot\left(\underset{\sim}{v}\frac{\partial F}{\partial E} + \underset{\sim}{v}_\perp \frac{1}{B}\frac{\partial F}{\partial \mu} + \underset{\sim}{n}\times\underset{\sim}{v}_\perp \frac{1}{v_\perp^2}\frac{\partial F}{\partial \phi}\right) - \frac{\partial f}{\partial \phi} = 0 \quad , \tag{2}$$

where $F = F_m + F^{(1)}$ is the equilibrium distribution function, ϕ is the gyrophase angle, E is the kinetic energy per unit mass, μ is the magnetic moment per unit mass, Φ is the perturbed electrostatic potential, and $\Omega \equiv eB/mc$. Species subscripts are suppressed here. We deal with a sheared magnetic field given by $\underset{\sim}{B} = B_z \underset{\sim}{e}_z + B_y(x)\underset{\sim}{e}_y$, and consider the ordering

$$\frac{k_\parallel}{k_\perp} = O(\varepsilon), \quad \frac{B_y}{B_z} = O(\varepsilon) \quad , \tag{3}$$

with ε being the fundamental smallness parameter and B_y taken to be proportional to x. Hence, $B \simeq B_z$, and $\underset{\sim}{n} \equiv \underset{\sim}{B}/B = \underset{\sim}{n}^{(0)} + \underset{\sim}{n}^{(1)}$, with $\underset{\sim}{n}^{(0)} = \underset{\sim}{e}_z$ and $\underset{\sim}{n}^{(1)} = (B_y/B)\,\underset{\sim}{e}_y$, where the superscripts

refer to the order in ϵ. Thus $n^{(1)}/n^{(0)} = O(\epsilon)$. F_m is a Maxwellian and, from Ref. 4,

$$F^{(1)} = \frac{v_\perp}{\Omega} \sin\phi \frac{\partial F_m}{\partial(\epsilon x)} \quad . \tag{4}$$

To lowest order in ϵ, Eq. (2) becomes

$$\underset{\sim}{v}_\perp \cdot \nabla^{(0)} f^{(0)} - \frac{e}{m} \nabla^{(0)} \phi^{(0)} \cdot \underset{\sim}{v}_\perp \frac{\partial F_m}{\partial E} - \Omega \frac{\partial f^{(0)}}{\partial \phi} = 0 \quad , \tag{5}$$

with the notation $\nabla_\perp^{(0)} = \partial/\partial \underset{\sim}{x}$, $\nabla_\perp^{(1)} = \partial/\partial(\epsilon x)$, and $\nabla_z = \nabla_z^{(1)} = \partial/\partial z$.
Defining $h^{(0)}$ by

$$f^{(0)} = \frac{e}{m} \phi^{(0)} \frac{\partial F_m}{\partial E} + h^{(0)} \quad , \tag{6}$$

Eq. (5) becomes

$$\underset{\sim}{v}_\perp \cdot \nabla^{(0)} h^{(0)} - \Omega \frac{\partial}{\partial \phi} h^{(0)} = 0 \quad . \tag{7}$$

Without loss of generality, we can express $h^{(0)}$ in the form:

$$h^{(0)} = (2\pi)^{-1/2} \int_{-\infty}^{\infty} dk_x \bar{h}(E, \mu, \phi, k_x) \exp i(k_x x + k_z z - \omega t) \quad . \tag{8}$$

Hence Eq. (7) becomes

$$(ik_x v_\perp \cos\phi + ik_y v_\perp \sin\phi - \Omega\partial/\partial\phi)\ \bar{h}\ \exp i\,(k_x x + k_y y) = 0 \quad . \tag{9}$$

Letting $\bar{h} = \hat{h}^{(0)}(E,\mu,k_x)g(\phi)$ gives

$$\frac{ik_x v_\perp}{\Omega}\ \cos\phi + \frac{ik_y v_\perp}{\Omega}\ \sin\phi = \frac{1}{g}\ \frac{\partial}{\partial\phi}\ g \quad , \tag{10}$$

so that

$$g(\phi) = \exp\left[i\frac{v_\perp}{\Omega}\ (k_x \sin\phi - k_y \cos\phi)\right] \quad . \tag{11}$$

From Eq. (8), we then get

$$n^{(0)} = (2\pi)^{-1/2} \int_{-\infty}^{\infty} dk_x \hat{h}^{(0)}\ (E,\mu,k_x)\ \exp i\,(k_x x + k_y y + k_z z - \omega t + L) \quad , \tag{12}$$

with $L = (v_\perp/\Omega)(k_x \sin\phi - k_y \cos\phi)$. Now we need to determine $\hat{h}^{(0)}$ from the first order form of Eq. (2), which becomes:

$$\frac{\partial f^{(0)}}{\partial t} + v_\parallel \underset{\sim}{n}^{(0)}\cdot\nabla^{(1)} f^{(0)} + v_\parallel \underset{\sim}{n}^{(1)}\cdot\nabla^{(0)} f^{(0)} + \underset{\sim}{v}_\perp\cdot\nabla^{(1)} f^{(0)} + \underset{\sim}{v}_\perp\cdot\nabla^{(0)} f^{(1)}$$

$$- e/m\nabla^{(0)}\phi^{(0)}\cdot\left\{\underset{\sim}{v}\ \frac{\partial F^{(1)}}{\partial E} + \underset{\sim}{v}_\perp\ \frac{1}{B}\ \frac{\partial F^{(1)}}{\partial\mu} + \underset{\sim}{n}^{(0)}\times\underset{\sim}{v}_\perp\ \frac{1}{v_\perp^2}\ \frac{\partial F^{(1)}}{\partial\phi}\right\}$$

$$- e/m\ \frac{\partial F_m}{\partial E}\left[\nabla^{(1)}\phi^{(0)}\cdot\underset{\sim}{v}_\perp + v_\parallel\left\{\underset{\sim}{n}^{(1)}\cdot\nabla^{(0)} + \underset{\sim}{n}^{(0)}\cdot\nabla^{(1)}\right\}\phi^{(0)}\right]$$

$$- \Omega\ \frac{\partial f^{(1)}}{\partial\phi} = 0 \quad . \tag{13}$$

In terms of $h^{(0)}$ this becomes

$$- i\omega h^{(0)} + \frac{e}{m}\frac{\partial \phi}{\partial t}^{(0)} \frac{\partial F_m}{\partial E} + v_{||}\underset{\sim}{n}^{(0)} \cdot \nabla^{(1)} h^{(0)} + v_{||}\underset{\sim}{n}^{(1)} \cdot \nabla^{(0)} h^{(0)}$$

$$+ \underset{\sim}{v}_{\perp} \cdot \nabla^{(1)} h^{(0)} + \frac{e}{m}\phi^{(0)} \underset{\sim}{v}_{\perp} \cdot \nabla^{(1)} \frac{\partial F_m}{\partial E} + \underset{\sim}{v}_{\perp} \cdot \nabla^{(0)} f^{(1)} - \frac{e}{m} \nabla^{(0)} \phi^{(0)}$$

$$\cdot \left\{ \underset{\sim}{v} \frac{\partial F}{\partial E}^{(1)} + \underset{\sim}{v}_{\perp} \frac{1}{B} \frac{\partial F}{\partial \mu}^{(1)} + \underset{\sim}{n}^{(0)} \times \underset{\sim}{v}_{\perp} \frac{1}{v_{\perp}^2} \frac{\partial F}{\partial \phi}^{(1)} \right\} - \Omega \frac{\partial}{\partial \phi} f^{(1)} = 0 \quad . \tag{14}$$

Again without loss of generality we can express $\phi^{(0)}$ in the form:

$$\phi^{(0)} = (2\pi)^{-1/2} \int_{-\infty}^{\infty} dk_x \hat{\phi}^{(0)}(k_x) \exp i\left(k_x x + k_y y + k_z z - \omega t\right) \quad . \tag{15}$$

Using Eq. (12) for $h^{(0)}$ and expressing $f^{(1)}$ in the form:

$$f^{(1)} = (2\pi)^{-1/2} \int_{-\infty}^{\infty} dk_x \hat{f}^{(1)}(E, \mu, \phi, k_x) \exp i\left(k_x x + k_y y + k_z z - \omega t + L\right) \quad , \tag{16}$$

Eq. (14) reduces to the following form after averaging over the gyrophase angle ϕ:

$$- i\omega\hat{h}^{(0)} + i\omega \frac{e\hat{\phi}^{(0)}}{T} F_m J_o\left(k_\perp v_\perp/\Omega\right) + ik_z v_{||}\, \hat{h}^{(0)}$$

$$+ ik_y v_{||} \frac{B_y}{B}\, \hat{h}^{(0)} + \frac{e}{m}\, \hat{\phi}^{(0)} \left\langle e^{-iL} \left\{ v_\perp \cos\phi \, \frac{\partial^2 F_m}{\partial E\, \partial(\epsilon x)} \right.\right.$$

$$- ik_x \left[v_\perp \cos\phi \left(\frac{\partial F^{(1)}}{\partial E} + \frac{1}{v_\perp} \frac{\partial F^{(1)}}{\partial v_\perp} \right) - \frac{1}{v_\perp} \sin\phi \, \frac{\partial F^{(1)}}{\partial \phi} \right]$$

$$\left.\left. + ik_y \left[v_\perp \sin\phi \left(\frac{\partial F^{(1)}}{\partial E} + \frac{1}{v_\perp} \frac{\partial F^{(1)}}{\partial v_\perp} + \frac{1}{v_\perp} \cos\phi \, \frac{\partial F^{(1)}}{\partial v_\perp} \right) \right] \right\} \right\rangle = 0 \quad , \tag{17}$$

where $k_\perp \equiv \left(k_x^2 + k_y^2\right)^{1/2}$, J_o is the usual Bessel function, and

$$\langle \cdot \cdot \cdot \rangle \equiv \frac{1}{2\pi} \int_0^{2\pi} d\phi \, \cdot \cdot \cdot \quad .$$

Substituting for $F^{(1)}$ from Eq. (4), the last term in Eq. (17) becomes

$$\frac{e}{m}\hat{\phi}(0)\left\langle e^{-iL}\left[v_\perp\cos\phi\ \frac{\partial^2 F_m}{\partial E\,\partial(\epsilon x)} - ik_x\frac{v_\perp^2}{\Omega}\cos\phi\sin\phi\ \frac{\partial^2 F_m}{\partial E\,\partial(\epsilon x)}\right.\right.$$

$$\left.\left. - ik_y\left(\frac{v_\perp^2}{\Omega}\sin^2\phi\ \frac{\partial^2 F_m}{\partial E\,\partial(\epsilon x)} + \frac{1}{\Omega}\frac{\partial F_m}{\partial(\epsilon x)}\right)\right]\right\rangle$$

$$= -\frac{e}{m}\hat{\phi}(0)\ \frac{ik_y}{\Omega}\ \frac{\partial F_m}{\partial(\epsilon x)}\ \left\langle e^{-iL}\right\rangle + \frac{e}{m}\hat{\phi}(0)\ \frac{\partial^2 F_m}{\partial E\,\partial(\epsilon x)}\ \left\langle e^{-iL}\right.$$

$$\left.\times\left[v_\perp\cos\phi - i\left(k_x\cos\phi + k_y\sin\phi\right)\frac{v_\perp^2}{\Omega}\sin\phi\right]\right\rangle$$

$$= -\frac{e}{m}\hat{\phi}(0)\ \frac{ik_y}{\Omega}\ \frac{\partial F_m}{\partial(\epsilon x)}\ J_o\left(\frac{k_\perp v_\perp}{\Omega}\right) + \frac{e}{m}\hat{\phi}(0)\ \frac{\partial^2 F_m}{\partial E\,\partial(\epsilon x)}$$

$$\times v_\perp\left\langle\frac{\partial}{\partial\phi}\left\{\sin\phi\ \exp\left[i\frac{v_\perp}{\Omega}\left(k_y\cos\phi - k_x\sin\phi\right)\right]\right\}\right\rangle$$

$$= -\frac{e}{m}\hat{\phi}(0)\ \frac{ik_y}{\Omega}\ \frac{\partial F_m}{\partial(\epsilon x)}\ J_o\left(\frac{k_\perp v_\perp}{\Omega}\right) \quad .$$

So, Eq. (17) reduces to

$$\hat{h}(0) = \frac{e\hat{\phi}(0)}{T}\ F_m\ J_o\left(\frac{k_\perp v_\perp}{\Omega}\right)\left(\frac{\omega-\omega_\star^T}{\omega-k_\parallel v_\parallel}\right) \quad , \qquad (18)$$

with $k_{||} \equiv k_z + k_y B_y/B$, $\omega_*^T \equiv \omega_* [1 + \eta (mE/T - 3/2)]$, $\eta \equiv (d \ln T/dx)/(d \ln n/dx)$, $\omega_{*e} \equiv - k_y(cT/eBL_n)$ and $L_n \equiv -(d \ln n/dx)^{-1}$. With $\hat{h}^{(0)}$ thus determined, Eq. (12) yields:

$$\hat{h}^{(0)} = \frac{e}{T} F_m \left(\frac{\omega - \omega_*^T}{\omega - k_{||} v_{||}} \right) \exp i \left(k_y y + k_z z - \omega t \right) (2\pi)^{-1/2} \times \int_{-\infty}^{\infty} dk_x \, \hat{\phi}^{(0)}(k_x) \, J_o \left(\frac{k_\perp v_\perp}{\Omega} \right) \exp i \left(k_x x + L \right) . \quad (19)$$

Finally, the gyrophase-averaged perturbed distribution function can be expressed as

$$\left\langle f^{(0)} \right\rangle = - \frac{e\phi^{(0)}}{T} F_m + \frac{e}{T} F_m \left(\frac{\omega - \omega_*^T}{\omega - k_{||} v_{||}} \right) (2\pi)^{-1/2} \int_{-\infty}^{\infty} dk_x \times \hat{\phi}^{(0)}(k_x) \, J_o^2 \left(\frac{k_x v_\perp}{\Omega} \right) \exp i \left(k_x x + k_y y + k_z z - \omega t \right) . \quad (20)$$

If we write $B_y/B = x/L_s$ and take $k_z = 0$ (which is equivalent to a change in origion of x), then $k_{||} = k_y x/L_s \equiv k_{||}' x$.

We will use the notation $\phi^{(0)} = \tilde{\phi}(x) \exp i\,(k_y y - \omega t)$ for the perturbed electrostatic potential and $n_j^{(0)} = \tilde{n}_j(x) \exp i\,(k_y y - \omega t)$ for the perturbed density, where $j = i$ for ions with charge e and $j = e$ for electrons with charge $-e$. Carrying out the velocity space integrations of Eq. (20) gives

$$\tilde{n}_i = -\frac{en}{T_i}\left[\tilde{\phi}(x) + \left(\frac{1}{v_i k_\parallel' |x|}\, Z(\xi_i)(2\pi)^{-1/2} \int_{-\infty}^{\infty} dk_x \exp(ik_x x)\right.\right.$$

$$\times \left\{\left[\omega - \omega_{*i}\left(1 - \tfrac{3}{2}\eta_i\right)\right]\Gamma_0 - \omega_{*i}\eta_i\left[\Gamma_0 + b(\Gamma_1 - \Gamma_0)\right]\right\}$$

$$\left. - \frac{\omega_{*i}\eta_i}{v_i k_\parallel' |x|}\left[\xi_i + \xi_i^2 Z(\xi_i)\right](2\pi)^{-1/2} \int_{-\infty}^{\infty} dk_x \exp(ik_x x)\Gamma_0\right)$$

$$\left. \times (2\pi)^{-1/2} \int_{-\infty}^{\infty} dx \exp(-ik_x x)\tilde{\phi}(x)\right] , \qquad (21)$$

and

$$\tilde{n}_e = \frac{en}{T_e}\tilde{\phi}(x)\left[1 + \left(\frac{\omega - \omega_{*e}}{v_e k_\parallel' |x|}\, Z(\xi_e) + \frac{\omega_{*e}\eta_e}{v_e k_\parallel' |x|}\left[\tfrac{1}{2} Z(\xi_e)\right.\right.\right.$$

$$\left.\left.\left. - \xi_e - \xi_e^2 Z(\xi_e)\right]\right)\right] . \qquad (22)$$

Here $v_j \equiv (2T_j/m_j)^{1/2}$, $\xi_j \equiv \omega/(v_j k_\parallel' |x|)$, $\Gamma_{0,1} \equiv I_{0,1}(b)\exp(-b)$, I_0 and I_1 are modified Bessel functions of the first kind, $b \equiv (k_x^2 + k_y^2)\rho_i^2/2 \equiv b_x + b_y$, $\rho_i \equiv v_i/\Omega_i$, and Z is the usual plasma

dispersion function. In computing $\tilde{n}_e$, $k_\perp \rho_e = k_\perp v_e / \Omega_e$ has been assumed to be negligible. Although Eqs. (21) and (22) are valid only in the collisionless limit, the addition of electron collisions by means of a number-conserving Krook model is straightforward.

The equation to be solved for the normal modes is just the quasi-neutrality condition,

$$0 = n_e - n_i \quad . \tag{23}$$

This equation can be solved by means of a Ritz method. First $\tilde{\phi}(x)$ is decomposed into appropriate basis functions:

$$\tilde{\phi}(x) = \sum_{n=0}^{\infty} \tilde{\phi}_n h_n(x) \quad , \tag{24}$$

where

$$h_n(x) = H_n \left(\sigma^{1/2} k_y \hat{s} x\right) \exp\left(-\sigma k_y^2 \hat{s}^2 x^2/2\right) M_n^{-1/2} \quad , \tag{25}$$

$\hat{s} \equiv (q'r/q)$ is the usual shear parameter, H_n is the Hermite polynomial of order n, and $M_n \equiv (\pi/\sigma)^{1/2} 2^n n!$. The operator

$$\frac{T_e k_y \hat{s}}{en} \int_{-\infty}^{\infty} dx \; h_{n'}(x)$$

is then applied to Eq. (23) to give the matrix equation

$$\sum_{n=0}^{\infty} L_{nn'}(\omega)\tilde{\phi}_n = 0 \quad , \tag{26}$$

where

$$L_{nn'}(\omega) = \left(1 + \frac{T_e}{T_i}\right)\delta_{nn'} + k_y s \int_{-\infty}^{\infty} dx\, h_{n'}(x) \left[\frac{\omega - \omega_{*e}}{v_e k_{\|}'|x|} Z(\xi_e)\right.$$

$$+ \frac{\omega_{*e}\eta_e}{v_e k_{\|}'|x|}\left(\frac{1}{2}Z(\xi_e) - \xi_e - \xi_e^2 Z(\xi_e)\right)$$

$$+ \frac{T_e}{T_i}\left(\frac{1}{v_i k_{\|}'|x|} Z(\xi_i)\,(2\pi)^{-1/2} \int_{-\infty}^{\infty} dk_x \exp(ik_x x)\right.$$

$$\times \left\{\left[\omega - \omega_{*i}\left(1 - \frac{3}{2}\eta_i\right)\right]\Gamma_0 - \omega_{*i}\eta_i\left[\Gamma_0 + b(\Gamma_1 - \Gamma_0)\right]\right\}$$

$$- \frac{\omega_{*i}\eta_i}{v_i k_{\|}'|x|}\left[1 + \xi_i^2 Z(\xi_i)\right](2\pi)^{-1/2} \int_{-\infty}^{\infty} dk_x \exp(ik_x x)$$

$$\left.\left.\times \Gamma_0\right)\,(2\pi)^{-1/2} \int_{-\infty}^{\infty} dx \exp(-ik_x x)\right] \quad h_n(x) \quad . \tag{27}$$

In practice, the summation in Eq. (26) will be truncated to a finite number of terms, N. The complex constant σ in Eq. (25) can be adjusted to minimize N, with the requirement that $\mathrm{Re}(\sigma) > 0$, so that $\lim_{x \to \pm\infty} \tilde{\phi}(x) = 0$. The basis functions given in Eq. (25) have the useful property that their Fourier transforms

are known analytically[5], e.g.

$$(2\pi)^{-1/2} \int_{-\infty}^{\infty} dx \exp(-ik_x x)\, h_n(x) = \frac{(-i)^n}{\sqrt{2}k_y\hat{s}}\, h_n\left(\frac{k_x}{\sigma k_y^2 \hat{s}^2}\right) \qquad (28)$$

so that Eq. (27) can be rewritten as

$$L_{nn'}(\omega) = \left(1 + \frac{T_e}{T_i}\right) \delta_{nn'} + k_y\hat{s} \int_{-\infty}^{\infty} dx\, h_{n'}(x) \left\{ \frac{\omega - \omega_{*e}}{v_e k_{\parallel}' |x|}\, Z(\zeta_e) \right.$$

$$\times h_n(x) + \frac{\omega_{*e}\eta_e}{v_e k_{\parallel}' |x|} \left(\frac{1}{2} Z(\zeta_e) - \zeta_e - \zeta_e^2\, Z(\zeta_e) \right) h_n(x)$$

$$+ \frac{T_e}{T_i} \left[\frac{1}{v_i k_{\parallel}' |x|}\, Z(\zeta_i)\, (2\pi)^{-1/2} \int_{-\infty}^{\infty} dk_x \exp(ik_x x) \right.$$

$$\times \left\{ \left[\omega - \omega_{*i} \left(1 - \frac{3}{2}\eta_i\right) \right] \Gamma_0 - \omega_{*i}\eta_i \left[\Gamma_0 + b\,(\Gamma_1 - \Gamma_0) \right] \right\}$$

$$\left. - \frac{\omega_{*i}\eta_i}{v_i k_{\parallel}' |x|} \left(\zeta_i + \zeta_i^2\, Z(\zeta_i) \right) (2\pi)^{-1/2} \int_{-\infty}^{\infty} dk_x \exp(ik_x x)\, \Gamma_0 \right]$$

$$\left. \times \frac{(-i)^n}{\sigma^{1/2} k_y \hat{s}}\, h_n\left(\frac{k_x}{\sigma k_y^2 \hat{s}^2}\right) \right\} . \qquad (29)$$

Hence only the x and k_x integrals need to be performed numerically when evaluating $L_{nn'}$. The numerical method used is high order Gauss-Hermite quadrature[6]. However, for the electron x integration, a separate Gaussian quadrature formula is used in the inner layer

$x \equiv 2x_e \equiv 2|\omega|/(k_\parallel' v_e)$. The numerical method used to determine the eigenvalue of ω for a selected eigenfunction is exactly that described in detail in Ref. 7 for the corresponding toroidal problem.

The usual second-order differential equation may be obtained from Eq. (23) by expanding the Bessel functions in Eq. (21) through second order in $k_x\rho_i \ll 1$, leaving $k_y\rho_i$ arbitrary. Specifically

$$\Gamma_1(b) \approx \Gamma_0(b_y) + [\Gamma_1(b_y) - \Gamma_0(b_y)]\, b_x^2 ,$$

and

$$b[\Gamma_1(b) - \Gamma_0(b)] \approx b_y[\Gamma_1(b_y) - \Gamma_0(b_x)] - [\Gamma_0(b_y) + 2b_y[\Gamma_1(b_y) - \Gamma_0(b_y)]]b_x^2 .$$

With appropriate integrations by parts, the integrals in Eq. (21) may then be performed to yield the familiar second order differential equation[1-4] governing long radial wavelength drift eigenmodes.

III. ELECTRON DRIFT EIGENMODES

As noted in the preceding section, the spatial variations in the equilibrium quantities is taken to be much weaker than the variations on the scale of the perturbations. Within the framework of this familiar ordering it has been demonstrated that collisionless electron drift waves ("universal modes") are absolutely stable at long radial wave lengths in a sheared slab geometry.[8] However, for larger azimuthal wavenumbers ($k_y\rho_i \sim 1$), the corresponding tighter radial localization of the eigenmodes (discussed in Sec. I) forces a consideration of shorter radial wavelengths. Since the differential equation formulation breaks down as $k_x\rho_i \to 1$, it becomes necessary to solve the integral eigenmode equation to determine the behavior of these waves in the shorter wavelength part of the spectrum.

As described in Sec. II-B, we have developed a computer code which implements the basis function, or Ritz, method to solve the eigenmode equation of interest. For the analysis of universal modes, this numerical procedure is limited by the requirement that there are two distinctly different length scales in the problem. Specifically, it is necessary to choose a sufficient number of appropriate basis functions to cover both the small-scale region around the average electron resonance point, $x_e \equiv |\omega|/k_\parallel' v_e$, as well as the large-scale region out to the average ion resonance point, $x_i \equiv |\omega|/k_\parallel' v_i$. To properly determine the stability properties of these modes it has been emphasized in the differential equation studies[1] that it is

essential to account for the detailed behavior around the narrow electron resonance region. Since the ratio, $x_i/x_e = (m_i T_e/m_e T_i)^{1/2}$, is obviously very large, the required number of basis functions, N, becomes correspondingly prohibitive for realistic mass ratios. In particular, it is found that the largest ratio, x_i/x_e, that can be practically handled is roughly equal to $N^{1/2}$. Hence, in the cases studied by this numerical procedure, we are restricted to artificially small mass ratios.

As a check on the integral formulation code, we considered some moderate wavelength cases ($k_y\rho_i \sim 1$) which are near the limits of validity of the differential formulation. For a representative use with $m_i/m_e = 100$, $k_y\rho_i = 0.63$, $L_s/L_n = 100$, $T_e = T_i$, $\eta_e = \eta_i = 0$, and $\sigma = 1.33$, we obtained an eigenvalue of $\omega/\omega_{*e} = 0.2261 + i9.6\times10^{-3}$ using 120 basis functions. Although not as accurate, this result compares reasonably well with a differential shooting code calculation of the same case using 500 equally-spaced grid points in x.[9] Specifically, the shooting code result is $\omega/\omega_{*e} = 0.2294 + i\,5.0\times10^{-5}$. The even eigenfunction and its Fourier transform, $\tilde{\phi}(k_x)$, calculated by the integral formulation code for this case are shown on Fig. 1. Here it is seen that, as expected, the eigenfunction is evanescent beyond the ion Landau resonance region, $|x| > x_i$. It is also of interest to note that the Fourier transformed eigenfunction for this moderately short wavelength case is dominated by values of $k_x\rho_i$ around 2.

To illustrate the qualitative behavior of the universal mode of shorter wavelengths, we now consider a representative case with $m_i/m_e = 100$, $k_y\rho_i = 0.71$, $L_s/L_n = 56$, $T_e = T_i$, $\eta_i = \eta_e = 0$, and $\sigma = 0.76$. On Fig. 2, the eigenvalue ω (normalized to ω_{*e}) is shown as a function of N for one even eigenfunction. The results here demonstrate that as the proper number of basis functions required to describe the eigenfunction is approached, the corresponding eigenvalue becomes that of a damped normal mode. In this, as well as for all of the other cases examined, we have found no evidence for the development of unstable universal eigenmodes at the shorter radial wavelengths where differences between the integral and differential formulations are significant. It should be noted, however, that these results in themselves do not constitute a mathematical proof for the non-existence of unstable short wavelength universal modes.

The lack of numerical efficiency of the Ritz method procedure for dealing with the universal modes is not difficult to understand. Since the basis functions die off rapidly in x beyond the width of the highest-n basis function kept, their truncation effectively forces the eigenfunction to zero at a very short distance beyond this x-value. The requirement then is that this point must fall well outside the ion Landau damping region ($x \approx x_i$), where the wave energy is absorbed. If this criterion is not met, the artificial forcing of the eigenfunction to zero

introduces corresponding spurious reflection of the outgoing energy. As a result, incorrect positive growth rates of the type shown in Fig. 2 can be readily generated.

Motivated by the preceding considerations, we have also analyzed the integral equation problem by a WKB procedure. As described in detail in Ref. 10, this involved the introduction of an ordering in powers of $\epsilon \sim \rho_i/L_n$ far from the relevant turning points and in powers of $\epsilon^{1/3}$ close to such turning points. Matching the solutions in the different regions then leads to the familiar form of the phase-integral eigenvalue condition:

$$\int_{x_1}^{x_2} dx k_x(x,\omega) = (p + 1/2)\pi \tag{30}$$

where $p = 0, 1, 2, \ldots$ and $k_x(x,\omega)$ is determined by the solution of the lowest order dispersion relation:

$$\Gamma_0 \left[\left(k_x^2 + k_y^2\right)\frac{\rho_i^2}{2}\right] = -\frac{1 + \frac{T_e}{T_i} + \left(1 - \frac{\omega_{*e}}{\omega}\right)(\xi_e)Z(\xi_e)}{\left(\frac{T_e}{T_i} + \frac{\omega_{*e}}{\omega}\right)(\xi_i)Z(\xi_i)} \quad . \tag{31}$$

Temperature gradients are ignored here for simplicity, and the turning points, x_1 and x_2, are determined by

$$k_x(x_1,\omega) = k_x(x_2,\omega) = 0 \quad . \tag{32}$$

This generally leads to complex values for x_1 and x_2.

The phase-integral procedure outlined here has been numerically implemented[11] using an interactive code.[12] When the appropriate evanescent boundary conditions are imposed, there is again no evidence found for the existence of unstable eigenmodes at short wavelengths. However, as noted earlier, these numerical studies do not prove in a mathematically definitive sense that such modes cannot exist.

IV ION DRIFT EIGENMODES

Unlike the situation for universal modes, the application of the Ritz method to the integral equation problem for ion drift waves is quite efficient. The obvious reason is that the small-scale effects associated with the electron resonance region ($x = x_e$) are unimportant for these eigenmodes. This fact is clearly demonstrated by the differential equation studies of long wavelength ion temperature-gradient-driven drift instabilities. Results from a shooting code analysis of a typical case (with parameters $L_s/L_n = 20$, $T_e/T_i = 2$, $\eta_i = \eta_e = 2$, and $k_y\rho_i = 1$) are displayed in Fig. 3. Here the eigenvalue, ω, is calculated as a function of the mass ratio. For unrealistically large ratios, such as $m_e/m_i = 1/100$, the electron resonances can introduce substantial shifts in the eigenvalue. However, for realistic values, such as $m_e/m_i = 1/3672$ or $1/1836$, the eigenvalue is negligibly shifted from that obtained assuming purely adiabatic electrons, i.e. $m_e/m_i = 0$. Hence, to a very good

approximation, the non-adiabatic effects associated with electron resonances can be ignored for these modes.

Using the adiabatic response for electrons, $\tilde{n}_e = (e\tilde{\phi}/T_e)n$, and again considering the case described in preceding comments, we calculated the eigenvalue as a function of the azimuthal wave number k_y, or $b_y \equiv k_y^2 \rho_i^2/2$, with a shooting code. As illustrated on Fig. 4, the results are in agreement with earlier calculations[2] showing that the growth rate has a maximum near $b_y = 0.8$ and that the mode frequency continues to increase beyond $b_y = 1.0$. However, at such relatively short wavelengths the differential equation used to derive these results is no longer valid. In what follows we will consider only the proper integral equation analysis of these modes.

Since the present eigenmode problem has only one spatial scale of interest, the Ritz method proves to be very efficient for obtaining solutions to the governing integral equation. Taking the parameters of the previous case solved with the shooting code, we used $\sigma = 1.0$ and $N = 120$ in the integral formulation code to obtain the eigenvalue, $\omega/\omega_{*e} = \omega\tau_s = -0.036 + i0.029$, for $b_y = 0.5$ (i.e., $k_y\rho_i = 1.0$). The differential equation result, $\omega/\omega_{*e} = -0.043 + i0.043$, differs by about 20% in the real frequency and 50% in the growth rate. Agreement between results from the two codes is, of course, better at longer wavelengths. In the present case, however, it can be concluded that the non-negligible shifts in the eigenvalue are due to inaccuracies introduced by the

differential approximation. This point is best illustrated by Fig. 5, where the corresponding even eigenfunction and its Fourier transform, $\phi(k_x)$, are plotted for this case. Although the root-mean-square value of $k_x\rho_i$ is of the same order as $k_y\rho_i \sim 1$, it is clear from Fig. 5 that the actual distribution in k_x for this mode extends to several times k_y with appreciable amplitude.

The dependence of the eigenvalue, ω, on the azimuthal wavenumber (b_y) and the ion-temperature gradient (η_i) has also been investigated with the integral formulation code. On Fig. 6 it is seen that the maximum growth rate occurs for b_y between 0.4 and 0.5, and that the real frequency, $-\omega_r\tau_s$, reaches a plateau at $b_y \gtrsim 0.7$. This differs significantly from the differential formulation results displayed in Fig. 4 which indicated maximum growth at $b_y \simeq 0.8$ and a continuing increasing trend for the real frequency beyond $b_y = 1.0$. On the other hand, the integral equation results for the η_i dependence of the eigenvalue displayed in Fig. 7 is in general qualitative agreement with the differential equation analysis. Both types of calculations indicate an instability threshold at $\eta_i \gtrsim 1$.

V. CONCLUSION

In this paper we have presented a systematic derivation of the appropriate integral eigenmode equation for analyzing drift waves of arbitrary radial wavelengths in a sheared slab system. For collisionless electron drift waves ("universal" modes) our main conclusion is that although we cannot definitely

rule out the possible existence of short wavelength absolute instabilities of this type, no evidence has been found to support their existence. As a practical point we should also note that the Ritz method is inefficient for dealing with the universal mode problem because of the stringent requirement that the basis functions used must properly cover the two widely different spatial scales associated with the electron and ion resonance regions. However, for the ion-temperature-gradient-driven ion drift instabilities, the Ritz procedure is quite efficient and allows us to readily explore the behavior of these modes throughout the spectrum. This is due to the fact that the electron resonance effects can be ignored for these instabilities. Our main conclusions for the η_i modes are: (1) even at short wavelengths ($k_y\rho_i \gtrsim 1$), the instability threshold remains at $\eta_i \gtrsim 1$; (2) the maximum growth rate for these modes occurs around $k_y\rho_i \simeq 1$; and (3) the real frequency reaches a plateau near $k_y\rho_i \gtrsim 1$ instead of following the monotonically increasing trend exhibited by the differential equation results.

ACKNOWLEDGMENTS

We would like to thank R. B. White for the use of his interactive WKB-shooting code.

This work was supported by the United States DoE Contract No. EY-76-C-02-3073.

REFERENCES

1. D. W. Ross and S. M. Mahajan, Phys, Rev. Lett. 40, 324 (1978); K. T. Tsang, P. J. Catto, J. C. Whitson, and J. Smith, Phys. Rev. Lett. 40, 327 (1978); L. Chen, P.N. Guzdar, R.B. White, P.K. Kaw, and C. Oberman, Phys. Rev. Lett. 41, 649 (1978).

2. R. E. Waltz, W. Pfeiffer, and R. R. Dominquez, General Atomic Report GA-A 15147 (1978).

3. W. M. Tang, R. B. White, and P. N. Guzdar, Princeton University Plasma Physics Laboratory Report PPPL-1541 (1979).

4. W. M. Tang, Nucl. Fusion 18, 1089 (1978).

5. E. C. Titchmarsh, Introduction to the Theory of Fourier Integrals (Clarendon, London, 1948), p. 81.

6. A. H. Stroud and D. Secrest, Gaussion Quadrature Formulas (Prentice Hall, Englewood Cliffs, 1966).

7. G. Rewoldt, W. M. Tang, and E. A. Frieman, Phys. Fluids 21, 1513 (1978).

8. T. Antonsen, Phys. Rev. Lett. 41, 33 (1978).

[9] D. Ross, Private Communication (1978).

[10] E. A. Frieman, G. Rewoldt, W. M. Tang, and A. H. Glasser, Princeton University Plasma Physics Laboratory Report PPPL-1560 (1979).

[11] W. W. Lee, Private Communication (1978).

[12] R. B. White, J. Comput. Phys. 31, 409 (1979).

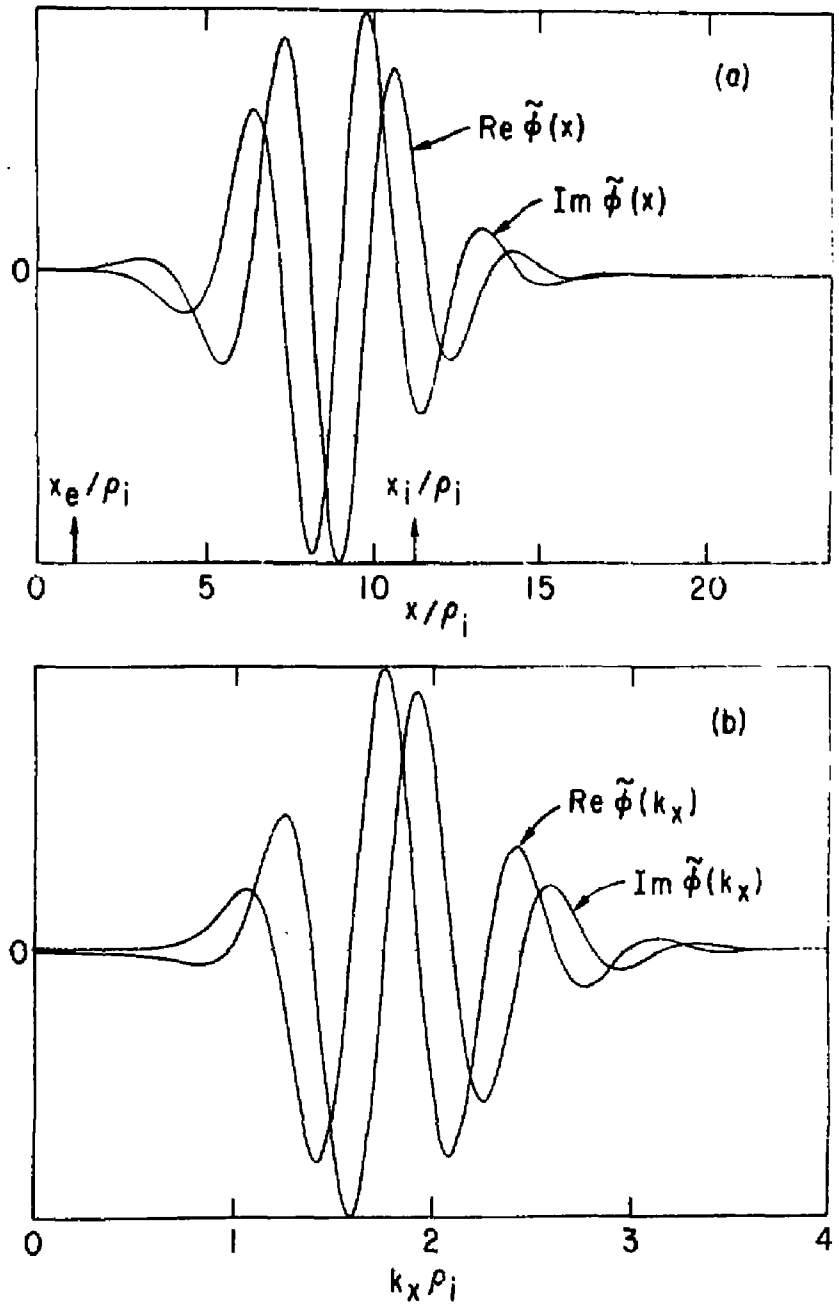

792324

Fig. 1. Eigenfunction $\tilde{\phi}(x)$ and Fourier transform $\tilde{\phi}(k_x)$ from the integral formulation code for the parameters: $k_y\rho_i = 0.63$, $L_s/L_n = 100$, $m_i/m_e = 100$, $T_e/T_i = 1$, $n_i = n_e = 0$, $\sigma = 1.33 + 0i$, and $N = 120$. The eigenvalue is $\omega/\omega_{*e} = 0.2261 + 0.0096i$.

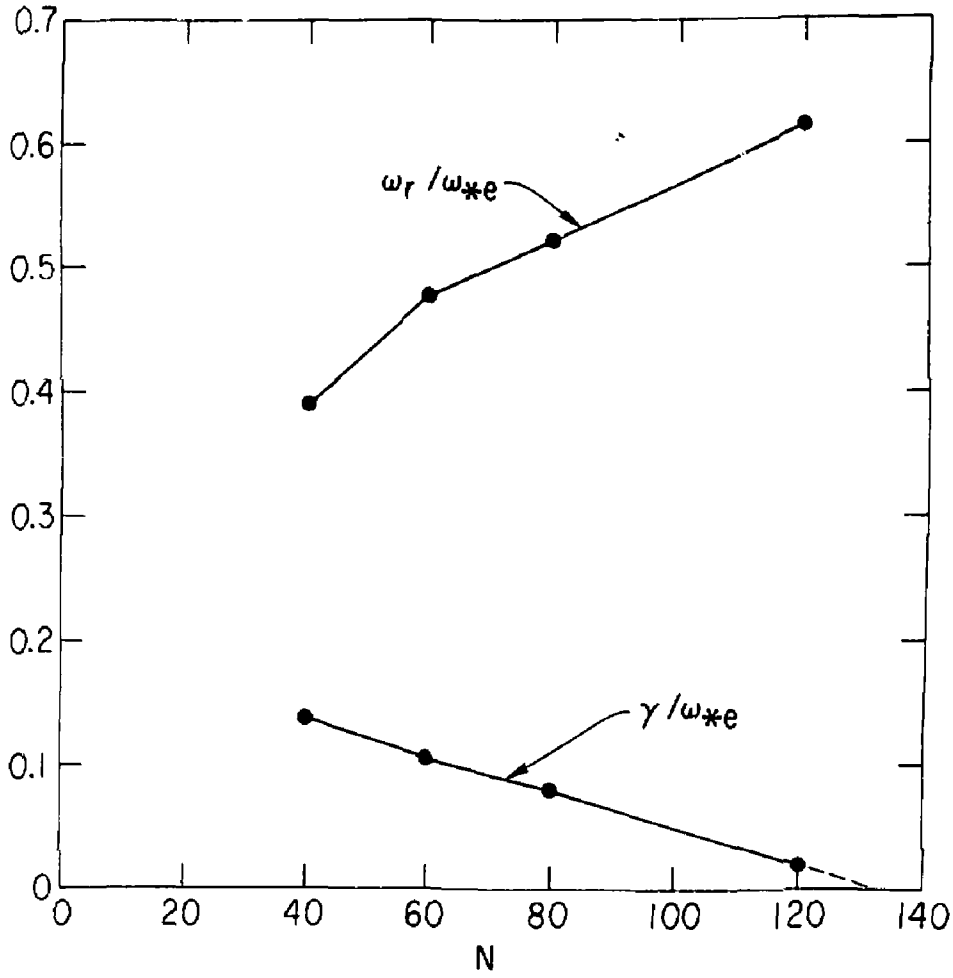

792312

Fig. 2. Real and imaginary parts of the eigenvalue $\omega \equiv \omega + i\gamma$ versus N, the number of basis functions used in the integral formulation code. The parameters are: $k_y\rho_i = 0.71$, $L_s/L_n = 56$, $m_i/m_e = 100$, $T_e/T_i = 1$, $\eta_i = \eta_e = 0$, and $\sigma = 0.76 + 0i$.

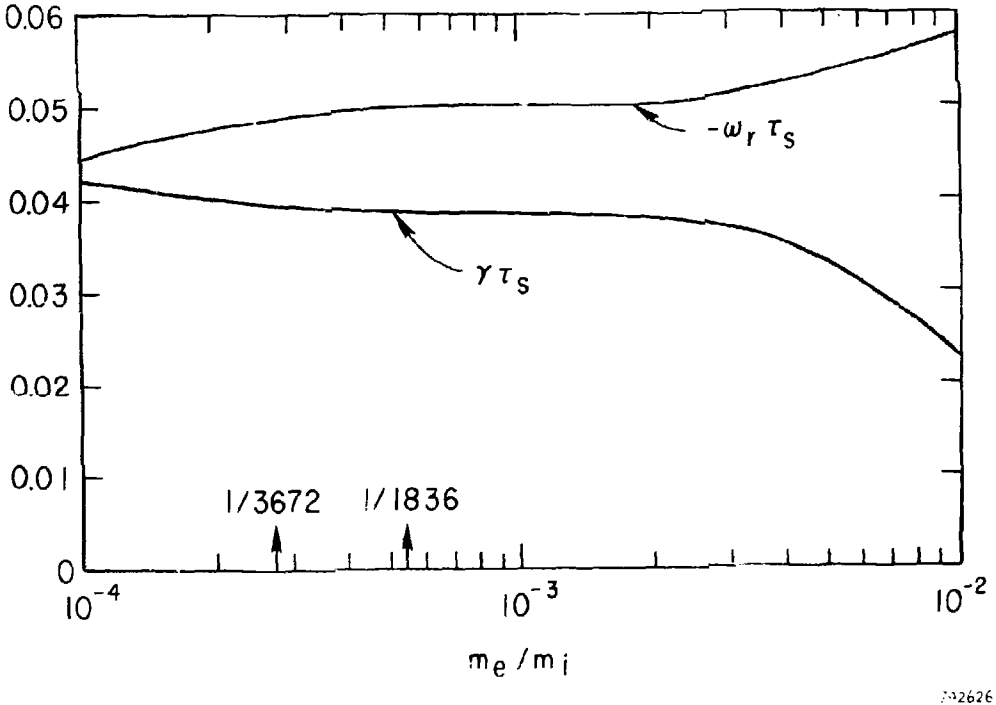

792626

Fig. 3. Mass-ratio dependence of the eigenvalues in the [illegible] for the parameters $k_y r_i = 1$, $L_s/L_n = 20$, $T_e/T_i = 2$, and [illegible].

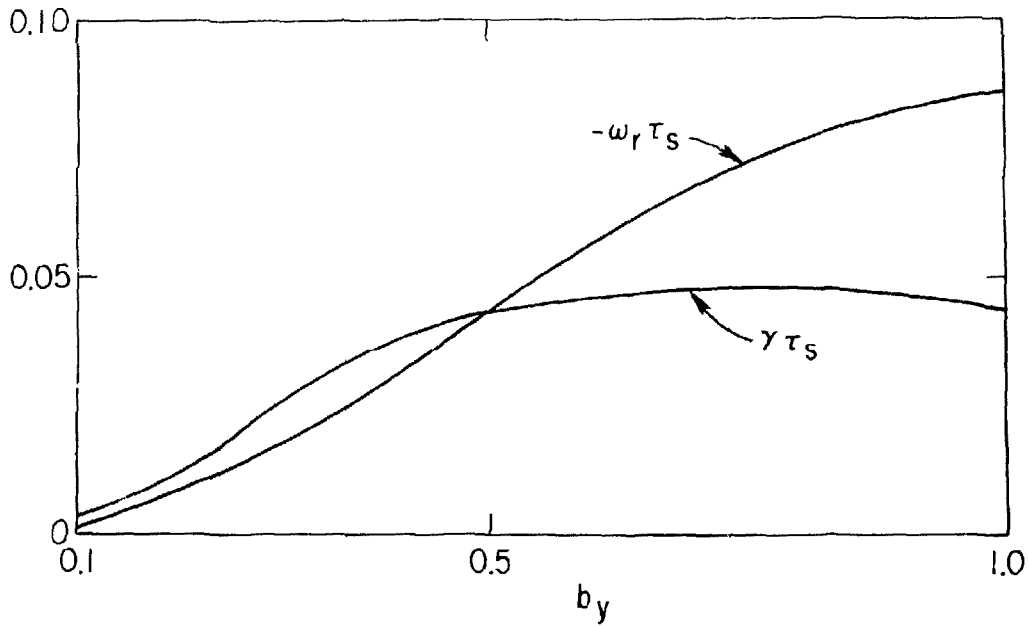

Fig. 4. Dependence of the eigenvalue ω on $b_y \equiv k_y^2 \rho_i^2/2$ in the differential approximation with adiabatic electron response for the parameters $L_s/L_n = 20$, $T_e^Y/T_i = 2$, and $\eta_i = 2$.

792459

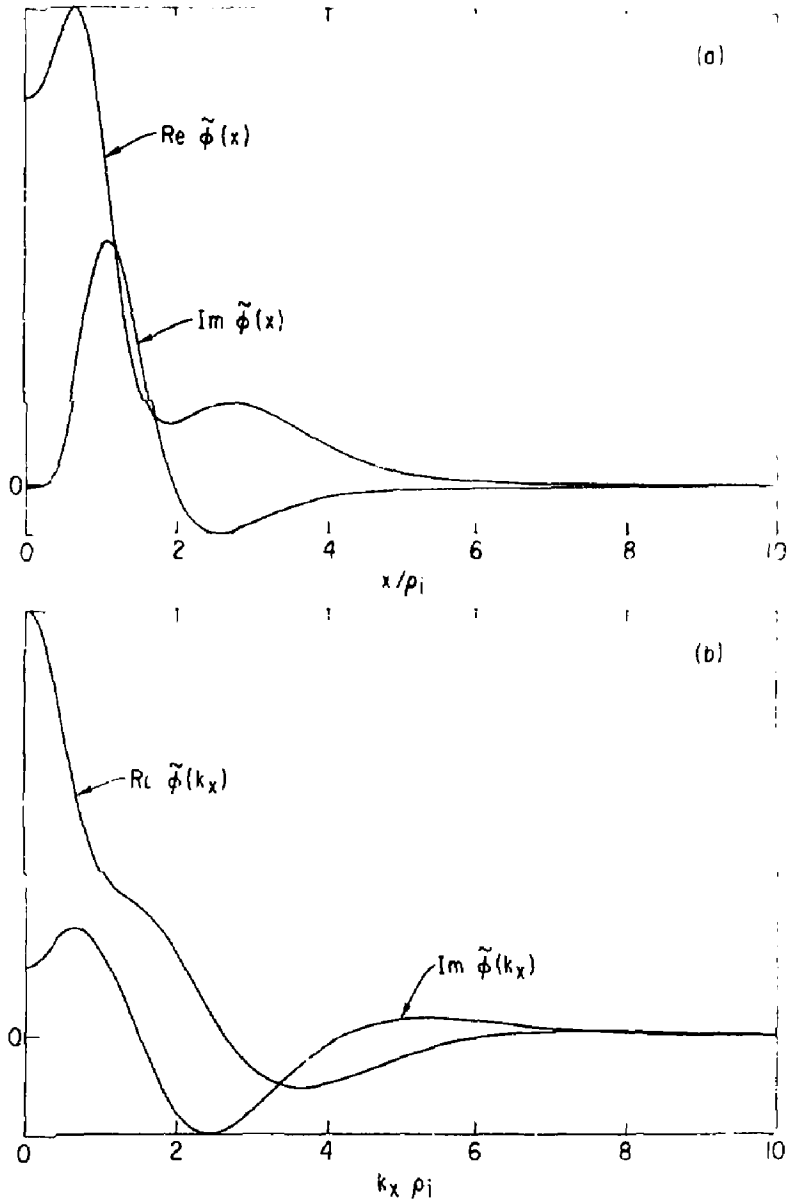

792546

Fig. 5. Eigenfunction $\tilde{\phi}(x)$ and Fourier transform $\tilde{\phi}(k_x)$ in the integral formulation with adiabatic electron response for parameters: $\hat{b}_y = 0.5$, $L_s/L_n = 20$, $T_e/T_i = 2$, $\eta_i = 2$, $\sigma = 1 + 0i$, and $N = 120$. The eigenvalue is $\omega/\omega_{*e} = -0.836 + 0.029i$.

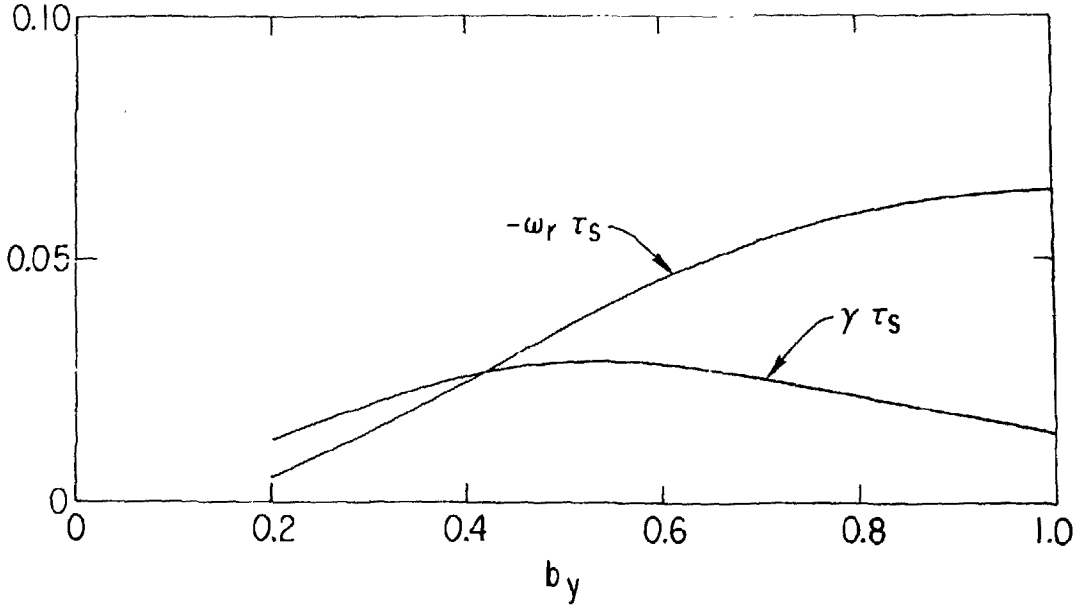

Fig. 6. Real and imaginary parts of the eigenvalue $\omega = \omega_r + i\gamma$ from the integral formulation code with adiabatic electron response, with the parameters: $L_n/L_T = 20$, $T_e/T_i = 2$, $\tau_i = 2$, $\varepsilon = 1 + 0i$, N = 120, and varying $b_y = k_y^2 \rho_i^2/2$. Here $\tau_s = [T_e b_y/T_i]^{1/2}/\omega_{*e}$ is independent of b_y. 792311

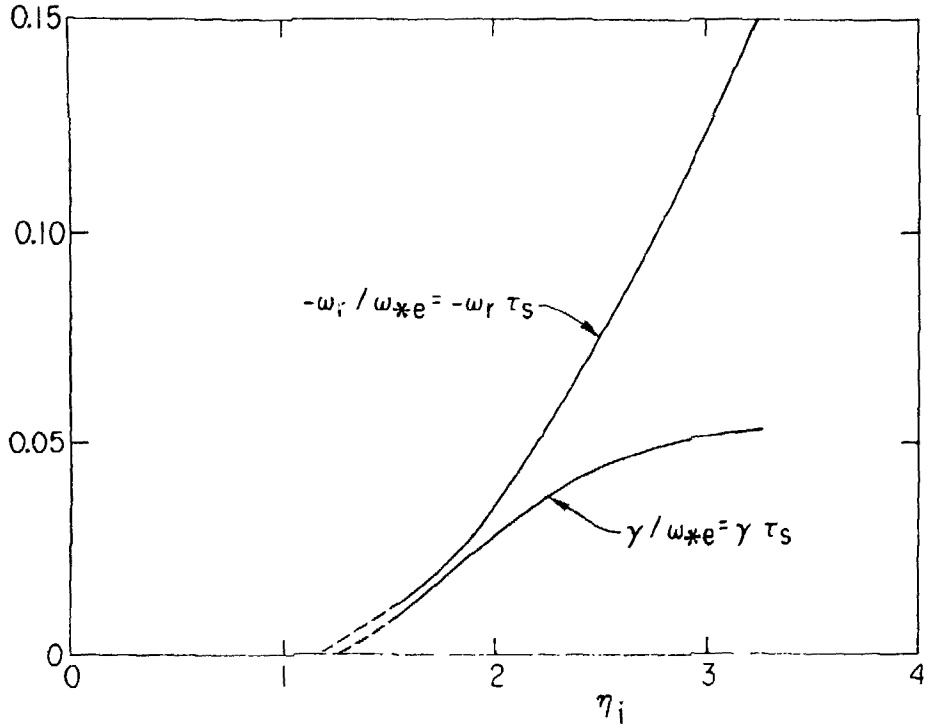

Fig. 7. Real and imaginary parts of the eigenvalue $\omega = \omega_r + i\gamma$, from the integral formulation code with adiabatic electron response, with the parameters: $L_s/L_n = 2.5$, $T_e/T_i = 2$, $k_\perp = 0.4$, $\epsilon = 1/20$, $N = 120$, and varying η_i.

782313